Development of atopic dermatitis-like skin disease from the chronic loss of epidermal caspase-8

Christopher Li[a], Samuel Lasse[a], Pedro Lee[a], Manando Nakasaki[a], Shih-Wei Chen[a], Kenshi Yamasaki[b], Richard L. Gallo[b], and Colin Jamora[a,b,1]

[a]Division of Biological Sciences, Section of Cell and Developmental Biology, and [b]Department of Medicine, Division of Dermatology, School of Medicine, University of California at San Diego, La Jolla, CA 92093

Edited by Elaine Fuchs, The Rockefeller University, New York, NY, and approved November 3, 2010 (received for review July 7, 2010)

Atopic dermatitis is an inflammatory skin disease that affects approximately 20% of children worldwide. Left untreated, the barrier function of the skin is compromised, increasing susceptibility to dehydration and infection. Despite its prevalence, its multifactorial nature has complicated the unraveling of its etiology. We found that chronic loss of epidermal caspase-8 recapitulates many aspects of atopic dermatitis, including a spongiotic phenotype whereby intercellular adhesion between epidermal keratinocytes is disrupted, adversely affecting tissue architecture and function. Although spongiosis is generally thought to be secondary to edema, we found that suppression of matrix metalloproteinase-2 activity is sufficient to abrogate this defect. p38 MAPK induces matrix metalloproteinase-2 expression to cleave E-cadherin, which mediates keratinocyte cohesion in the epidermis. Thus, the conditional loss of caspase-8, which we previously found to mimic a wound response, can be used to gain insights into how these same wound-healing processes are commandeered in inflammatory skin diseases.

inflammation | adherens junction | T cells | eczema

The theory that processes functioning during a wound healing response underlie many inflammatory diseases is a classic hypothesis. Among the first to describe this connection was Rudolf Virchow, who, in 1863, correlated tumorigenesis with past episodes of injuries and irritations (1). The wound-healing program in the skin is a highly regulated series of interdependent events that restore tissue homeostasis following an injury. Among the initial responses following trauma is inflammation wherein immune cells infiltrate the tissue to ward off invading microbes. This is followed by the proliferation of stem/progenitor cells to provide the materials to replace lost or damaged tissue. Finally, there is remodeling of cell and tissue architecture to integrate the new structures in the context of the preexisting tissue. Many diseases, including cancer, appear to usurp and deregulate the inflammatory, proliferative, and tissue remodeling phases of the wound response (2), endowing them with a "wound signature." Thus, understanding the normal wound healing process may shed light on how it is deregulated to cause a pathological condition.

We previously found that transient down-regulation of epidermal *caspase-8* is sufficient to recapitulate a wound healing response in the absence of trauma to the skin (3). Interestingly, among the reported symptoms in humans with a systemic deficiency of *caspase-8* is the inflammatory skin disease eczema (4). A common type of eczema is atopic dermatitis (AD), the hallmarks of which are chronic inflammation, disruption of epidermal barrier function, immunological abnormalities, and increased serum IgE, all of which results from a complicated interplay between genetic and environmental factors (5). The multiple cell types and reciprocal signaling pathways involved in manifesting these clinical features have made understanding its cause and combating its effects a challenging endeavor. One difficulty in unraveling these networks is distinguishing the causative and promoting factors from the processes that are the result of disease-specific modifications. The impetus for understanding AD is borne from the fact that, within the past decade, its incidence has been increasing and now affects 15% to 30% of children in the world (6). The danger posed by this progressive disease is the impairment of the barrier function of the skin, which protects the body from environmental microbes and toxins as well as maintain the body's hydration. The wound signature of AD (1, 2) is chronic inflammation, proliferation of progenitor cells leading to epidermal hyperplasia, and tissue remodeling resulting in the development of spongiosis. The spongiotic defect is a morphological feature that describes the separation of keratinocytes in the epidermis, which disrupts the architecture of the tissue.

In addition to cutaneous inflammation, patients with a genetic deficiency of caspase-8 also exhibited a plethora of defects in their adaptive immune system (4). This is consonant with the proposition that disruption of elements of the physical barrier along with abnormalities in T cell homeostasis and perturbation in the cytokine network are important pathogenic factors in the development of inflammatory skin diseases such as AD (7). However, patients with AD do not possess the entire palette of phenotypes resulting from the systemic deficiency of caspase-8, suggesting that a more tissue-restricted defect in caspase-8 expression may underlie this disease. Given the similarities between AD and a chronic wound healing response, we set out to test the hypothesis that the genetic ablation of *caspase-8* specifically in the epidermis can be used as a system to understand certain aspects of this disease.

Results

Histopathology of Caspase-8–Null Skin. Analysis of human AD skin revealed a decrease in the levels of caspase-8 in the epidermis (Fig. 1*A* and Fig. S1). To determine the specific contribution of epidermal caspase-8 reduction to this pathologic process, we investigated the extent to which the diagnostic profile for AD is represented in the mutant mouse. Similar to patients with AD (8) the *caspase-8* conditional KO (C8 cKO) mouse exhibits dry and scaly skin (Fig. 1*B*), as well as a thickened (acanthotic) epidermis (Fig. S2). The latter is partly caused by the hyperproliferation of epithelial stem/progenitor cells in the skin and alterations in the differentiation program of epidermal keratinocytes (3).

Examination of the ears and feet of the C8 cKO mouse revealed evidence of cutaneous edema (Fig. 1*C* and Fig. S3). This accumulation of interstitial fluid correlates with an approximate

Author contributions: C.J. designed research; C.L., S.L., P.L., M.N., S.-W.C., K.Y., and C.J. performed research; R.L.G. contributed new reagents/analytic tools; C.L., S.L., P.L., R.L.G., and C.J. analyzed data; and R.L.G. and C.J. wrote the paper.

The authors declare no conflict of interest.

This article is a PNAS Direct Submission.

Freely available online through the PNAS open access option.

[1]To whom correspondence should be addressed. E-mail: cjamora@ucsd.edu.

This article contains supporting information online at www.pnas.org/lookup/suppl/doi:10.1073/pnas.1009751108/-/DCSupplemental.

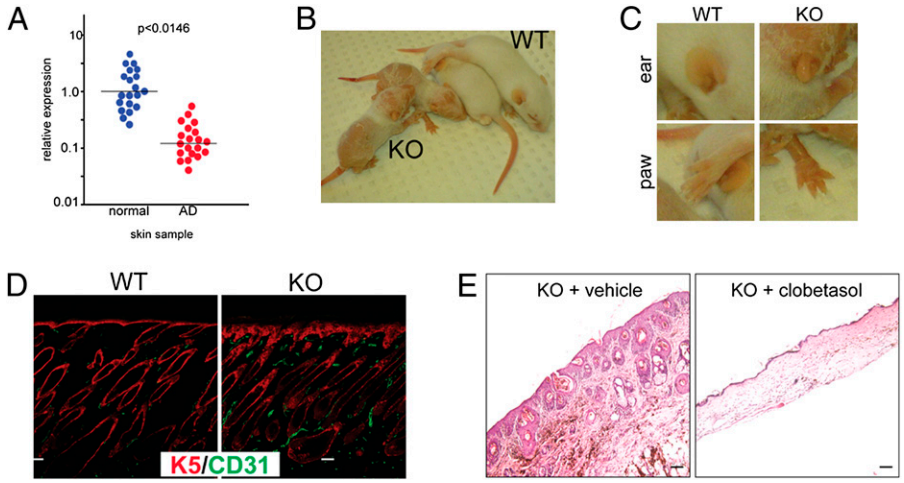

Fig. 1. AD characteristics in C8 cKO mice. (*A*) Expression of caspase-8 in normal and human AD skin measured by quantitative PCR. (*B*) Appearance of WT and C8 cKO at postnatal day 10. (*C*) Appearance of ears and paws in WT and KO animals. (*D*) Blood vessel population denoted by CD31 staining (green) in the WT and KO skin stained with keratin 5 (K5; red). (*E*) H&E of caspase-8–null skin treated with vehicle control (KO + vehicle) or clobetasol (KO + clobetasol) twice daily for 10 d. (Scale bars, 30 μm.)

2.5 fold increase in the amount of blood vessels found in the mutant (Fig. 1*D* and Fig. S4). The inflammatory changes and epidermal hyperplasia in the C8 cKO mouse (3, 9) also place an added demand for angiogenesis.

A typical regimen for the treatment of human AD is the topical application of a corticosteroid, a common one being clobetasol propionate (10). Similar to its effect on human AD skin, topical application of clobetasol substantially reduced the epidermal hyperplasia in the C8 cKO mouse (Fig. 1*E*).

Immunopathogenesis of Caspase-8–Null Skin. We next focused our investigation on whether the signature immune response in patients with AD is recapitulated in the C8 cKO mouse. The immune profile in patients with AD is a biphasic response of two subsets of $CD4^+$ helper T cells. During the acute phase of AD, the specific subset of $CD4^+$ T cells that are present belong to the T_H2 lineage. Consistent with this, we found that the skin of the C8 cKO mouse had maximal levels of T_H2 markers relative to the WT skin in young (10 d old) mice (Fig. 2*A* and Fig. S5*A*), and

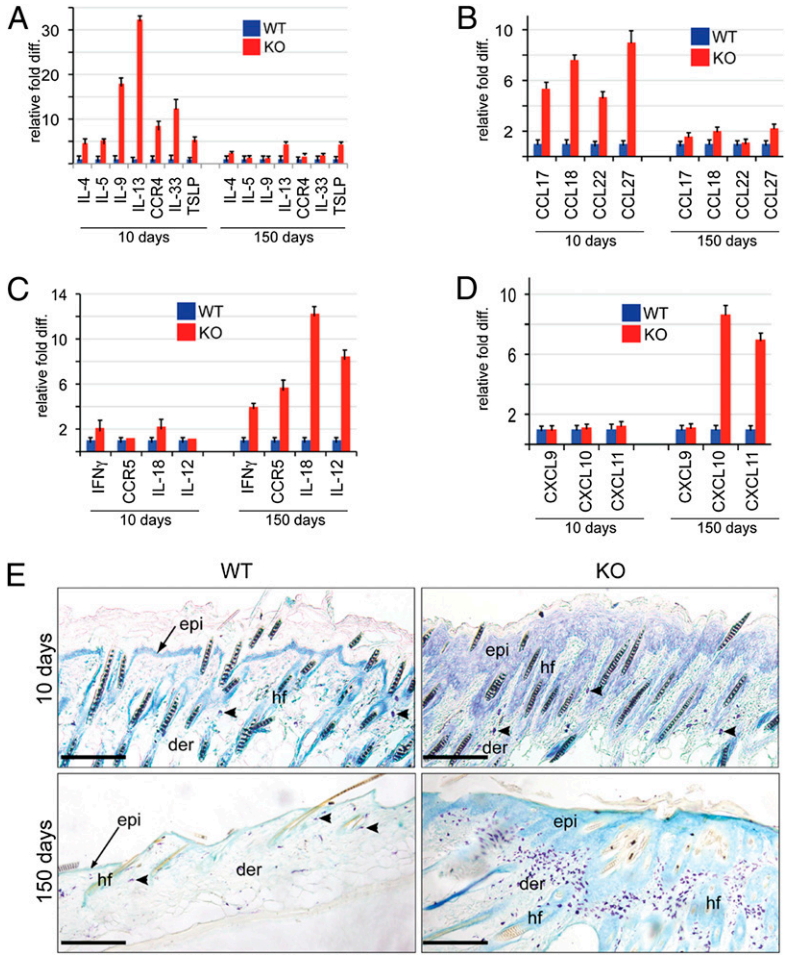

Fig. 2. Immune cell profile in C8 CKO skin. Representative quantitative RT-PCR on three sets of skin samples from WT (blue) and KO (red) 10-d- or 150-d-old mice wherein WT samples were normalized to one. Error bars are SEM of experiments performed in triplicate. (*A*) T_H2 signature genes. (*B*) T_H2 chemokines. (*C*) T_H1 signature genes. (*D*) T_H1 chemokines. (*E*) Toluidine blue staining of 10-d- or 150-d-old skin from WT and KO mice. Epidermis (epi) and hair follicle (hf) are shown in blue and mast cells in the dermis (der) are shown in purple. Arrowhead indicates mast cells. (Scale bars, 30 μm.)

these elevated levels waned as the animal aged. These signature genes include cytokines secreted from these cells such as *IL-4*, *IL-5*, *IL-9*, and *IL-13* (11), as well as the *chemokine receptor 4*, which is preferentially expressed on the surface of T_H2 cells (12). Consistent with a role for T_H2 cells in the pathogenesis of the C8 cKO skin, we found that *IL-33* is also elevated (Fig. 2*A*). Moreover, there is a moderate increase of *thymic stromal lymphopoietin (TSLP)* levels in the C8 cKO skin (Fig. 2*A*). Interestingly, transgenic mice engineered to overexpress *IL-4*, *IL-13*, *IL-33*, or *TSLP* all result in an AD-like phenotype (8).

Given the impact of T_H2 cells in the acute phase of the pathogenesis of AD, we investigated the mechanism responsible for the recruitment of T cells into the C8 cKO skin. We observed that the *chemokine (C-C motif) ligand (CCL)-22* secreted from dendritic cells, *CCL18* produced by dendritic cells and keratinocytes, *CCL27* from keratinocytes, and *CCL17* from dendritic cells and endothelial cells are up-regulated in the C8 cKO skin (Fig. 2*B* and Fig. S5*A*). These same CCLs have likewise been implicated in the recruitment of T cells into atopic skin (13). Consistent with the role of T_H2 cells in the acute phase of AD, the chemokines that recruit them are highest in young mice and decrease as the mice age.

The chronic phase of the immune response in patients with AD is marked by the appearance of T_H1 cells (5). The signature genes for this subset of T helper cells include *IFN-γ* and *chemokine receptor 5*, both of which are not substantially altered in young C8 cKO mice but are elevated in adult skin (Fig. 2*C*). Although the increase in *IFN-γ* gene expression in the adult is modest, it translates into a substantial increase in the amount of secreted protein from the C8 cKO epidermis (Fig. S5). IFN-γ can stimulate keratinocytes to produce and secrete IL-18 (11), which is also found to be up-regulated in the C8 cKO skin of adult mice (Fig. 2*C*). Interestingly, IL-18 is elevated in the serum of patients with AD (14) and transgenic overexpression of this cytokine in epidermal keratinocytes closely models the human disease (15). Recruitment of T_H1 cells to the adult C8 cKO skin is likely the consequence of the up-regulation of the chemokines *CXCL10* and *CXCL11* (Fig. 2*D*). Additionally, IFN-γ activates resident dendritic cells as well as macrophages to secrete IL-12, which is enriched in chronic skin lesions in patients with AD (16) and, together with IL-18, skew the immune response toward T_H1 polarization.

One consequence of this T cell signaling is the recruitment and activation of mast cells, which contribute to the inflammatory processes facilitating AD progression (17). In both young and adult C8 cKO mice, there is an elevated number of mast cells that increases as the animal ages (Fig. 2*E* and Table S1).

Serum Ig Levels. Among the diagnostic features of AD are elevated levels of IgG1 and IgE in the serum of patients. Increased serum IgG1 levels can be detected in young C8 cKO mice and culminates in a approximately fivefold increase in the adult C8 cKO mouse relative to its WT littermate (Fig. 3*A*). In early infancy, AD appears as the non–IgE-associated form (5), but the majority of patients with AD develop elevated serum IgE later in life. Consistent with the progression of AD in humans, there is no difference in IgE levels in young mice, but adult C8 cKO mice display an approximately 30-fold increase relative to its WT littermate (Fig. 3*B*). These IgEs can bind to their high affinity receptor on mast cells (Fig. 2*E*) and stimulate them to degranulate and release cytokines that mediate various allergies and development of asthma (18).

Development of Spongiosis in the Caspase-8–KO Epidermis. One of the histological signs of AD is the impairment of intercellular adhesions between epidermal keratinocytes, resulting in the formation of gaps known as spongiosis (19). Approximately 90% of the C8 cKO mice with a uniform phenotype throughout its body surface die by postnatal day 15. However, 10% of the mice

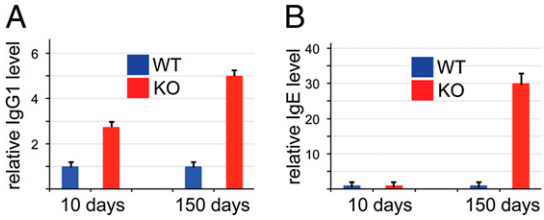

Fig. 3. Serum levels of Ig from WT (blue) and C8 cKO (red) were determined by ELISA. (*A*) IgG1 levels and (*B*) IgE levels in 10-d- and 150-d-old mice. Results are representative of three sets of mice performed in triplicate and error bars indicate SEM.

were mosaic and survived for months. The mosaicism manifested itself on the posterior region of the back skin, which had a phenotypic area of approximately 2.5 cm in diameter. We limited our analysis to the central portions of this region, where the phenotype is more homogenous relative to the periphery. Within these patches, suprabasal cells exhibited an increase in intercellular space yielding the characteristic sponge-like appearance (Fig. 4*A*). Interestingly, the restriction of this spongiotic phenotype to the suprabasal layers mimics the defect found in human AD skin (19).

The structural organization of the epidermis is largely established and maintained by intercellular adhesion apparatuses nucleated by the cadherin superfamily of proteins such as E-cadherin (20). We therefore examined E-cadherin expression and found that its normal localization as a thin line at the plasma membrane of keratinocytes in the suprabasal layers of the WT epidermis was primarily punctate in the C8 cKO mouse (Fig. 4*B*). This punctate staining pattern suggested that the E-cadherin was being shed from the cell surface and this was verified by the decrease in the full-length protein found in the C8 cKO skin (Fig. 4*C*). However, other components of adherens junctions and other intercellular adhesion proteins appear to be unaffected in the C8 cKO epidermis.

Given the effect on tissue structure, we tested whether the C8 cKO skin also displayed signs of compromised function. Mutations in the filaggrin gene, which encodes a protein critical for epidermal differentiation and barrier formation, is a predisposing factor in AD (21). Consistent with the human disease, the adult C8 cKO epidermis exhibits a substantial decrease in filaggrin protein levels (Fig. 4*D*). In addition to the loss of functional filaggrin, elevated TSLP expression has also been shown to correlate with the persistence of a barrier defect (22). Evidence of an impaired barrier function in the adult C8 cKO mouse is further suggested by an increased amount of TSLP secreted from the epidermis and found in circulating in the serum (Fig. 4*E*), which occurs in tandem with an increase in epidermal water loss (TEWL) in adult mice (Fig. 4*F*). Production of *TSLP* in keratinocytes is stimulated by inflammatory and T_H2 cytokines (23), and inhibition of this immune cell signaling via clobetasol treatment lowers both TSLP levels and epidermal water loss (Fig. 4 *E* and *F*).

Regulation and Function of Epidermal Matrix Metalloproteinase-2. To probe the underlying mechanism of the shedding of E-cadherin, we screened through various families of proteases whose members may be responsible for cleavage of the extracellular domain of cadherin such as matrix metalloproteinases (MMPs). Among the proteases that we observed to be up-regulated in the young C8 cKO mice are *MMP-2*, *MMP-9*, and *MMP-13* (Fig. 5*A*). As *MMP-13* is not found in human tissue, we focused on MMP-2, which has been localized in lesions of human AD skin, although its contribution to this disease remains undefined (24). *MMP-2* is not normally present in WT skin but is induced in the C8 cKO epidermis by p38 MAPK (Fig. 5*B*). Moreover, activation of p38

MEDICAL SCIENCES

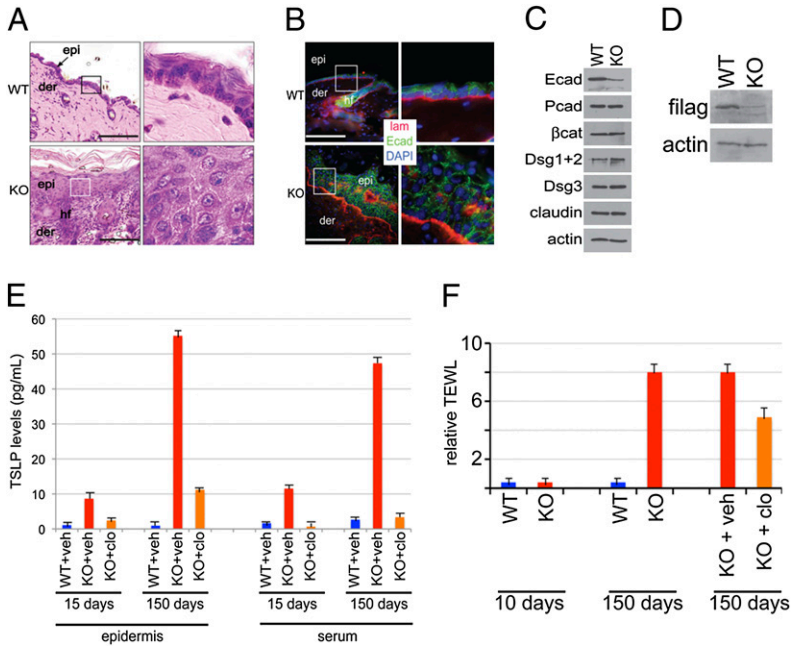

Fig. 4. C8 cKO mice have altered epidermal structure and function. (*A*) H&E staining of WT and KO skin from 5-mo-old mice. *Right*: Magnified views of boxed areas (*Left*). (*B*) Staining for E-cadherin (Ecad; green), laminin (lam; red) and nuclei (DAPI; blue) in WT and KO skin sections. Epi, epidermis; der, dermis; hf, hair follicle. *Right*: Magnified views of the boxed area (*Left*). (Scale bars, 30 μm.) Western blots using actin as a control on 5 mo WT and KO skin to detect intercellular adhesion proteins (*C*) and filaggrin (*D*). (*E*) TSLP levels secreted from the epidermis or in the serum of young (15 d) or adult (150 d) mice treated with vehicle control (veh) of clobetasol (clo). (*F*) Measurement of TEWL under similar conditions as *E*. Results are representative of three readings taken on different regions of the back from three sets of animals. Error bars indicate SEM.

MAPK is sufficient to induce *MMP-2* expression in keratinocytes in vitro (Fig. 5*C*). Upon observing an increase in *MMP-2* gene expression, we examined the protein levels of MMP-2, which is synthesized as an inactive zymogen that must be proteolytically cleaved to be activated. Although the protein is present in young C8 cKO animals, it is in its inactive state, and after reaching adulthood, the active form is generated (Fig. 5*D*). Moreover, although p38 MAPK can induce expression of MMP-2, it is not sufficient to activate the protein.

The relevance of MMP-2 to the integrity of adherens junctions was determined by testing the effect of this protease on the E-cadherin connecting epidermal keratinocytes in vitro. In mature adherens junctions, E-cadherin is stabilized at the interface of two cells and appears as an outline of the cell periphery by immunofluorescence (Fig. 5*E*). Incubation of these cells with activated recombinant MMP-2 resulted in punctate remnants of E-cadherin at the tips of filopodia-like structures that evoke the spongiotic phenotype of the C8 cKO epidermis. In contrast, treatment of keratinocytes with activated MMP-13 is unable to alter the organization of adherens junctions (Fig. S6). The shedding of E-cadherin was verified by Western blot (Fig. 5*F*). MMP-2 can decrease the amount of full length E-cadherin (Ecad FL) via cleavage of its ectodomain, resulting in an increase in the amount of E-cadherin C-terminal fragments (Ecad CTF) within the keratinocyte.

In light of the ability of p38 MAPK to induce MMP-2 expression, the question then arises of how the loss of caspase-8 activates this stress kinase. A clue to this mechanism was provided by a report demonstrating that inflammation is capable of activating p38 MAPK (25). Consistent with this, the anti-inflammatory effect of the corticosteroid clobetasol was able to abolish the expression of active p38 MAPK (Fig. 5*G*), thereby preventing the expression of MMP-2 and shedding of E-cadherin (Fig. 5*H*).

Role of MMP-2 in Spongiosis. The ability of active MMP-2 to alter intercellular adhesion in vitro led us to examine whether a similar phenomenon was occurring in the C8 cKO epidermis. Subcutaneous injection of MMP-2 inhibitor significantly reduced the intercellular space found in the suprabasal layers of the epidermis whereas the hyperproliferative phenotype remained unchanged (Fig. 6*A*). The potential off-target effects of the MMP-2 inhibitor on MMP-9 activity in the epidermis is not an issue, since *MMP-9* is expressed exclusively in the dermis of the C8 cKO mouse (Fig. 5*A*). Moreover, inhibition of MMP-13, which is also elevated in the C8 cKO skin (Fig. 5*A*), did not affect the spongiotic phenotype (Fig. S7*A*). On the contrary, clobetasol treatment not only reduced the epidermal hyperplasia but also abolished the epidermal gaps (Fig. S7*A*).

Repression of the spongiotic phenotype by the inhibition of MMP-2 activity suggested that the cleavage of E-cadherin was likewise suppressed in vivo. We performed Western blots on treated skin and found that inhibition of MMP-2 activity was able to restore Ecad FL to WT levels and significantly reduce the amount of the cleaved CTF product (Fig. 6*B*). Therefore, MMP-2 activity can significantly impact the status of the E-cadherin protein in the C8 cKO epidermis and, in so doing, influence the organization of this tissue.

The ability of the MMP-2 inhibitor to restore keratinocyte cohesion and tissue architecture prompted us to assess whether it can also affect the barrier function of the skin. Transepidermal water loss (TEWL) through the C8 cKO epidermis treated with the MMP2 inhibitor was dramatically reduced relative to DMSO-treated skin (Fig. 6*C*). Furthermore, inhibition of p38 MAPK activation (and therefore MMP-2 expression) via clobetasol treatment likewise significantly reduced TEWL in the C8 cKO skin. Altogether, these data suggest that the activity of MMP-2 can regulate both the structure and barrier function of the epidermis.

Discussion

The parallels between a chronic wound healing response and the features of AD encouraged us to investigate whether the prolonged repression of caspase-8 may contribute to this inflammatory disease. We found that the conditional deletion of epidermal caspase-8 recapitulates many of the clinical hallmarks of AD: epidermal thickening (acanthosis), scaling, elevated serum immunoglobulins, a biphasic T-helper cell response, mast cell infiltration, and spongiosis (8). As outlined in Table S1, the deletion of epidermal caspase-8 simulates the temporal progression of AD remarkably well. Moreover, the genetic ablation of epidermal caspase-8 causes changes in the expression of downstream genes seen in multiple mouse models of AD (Fig. S8). One notable difference between the caspase-8 model and human AD is the late onset of the spongiotic phenotype in the

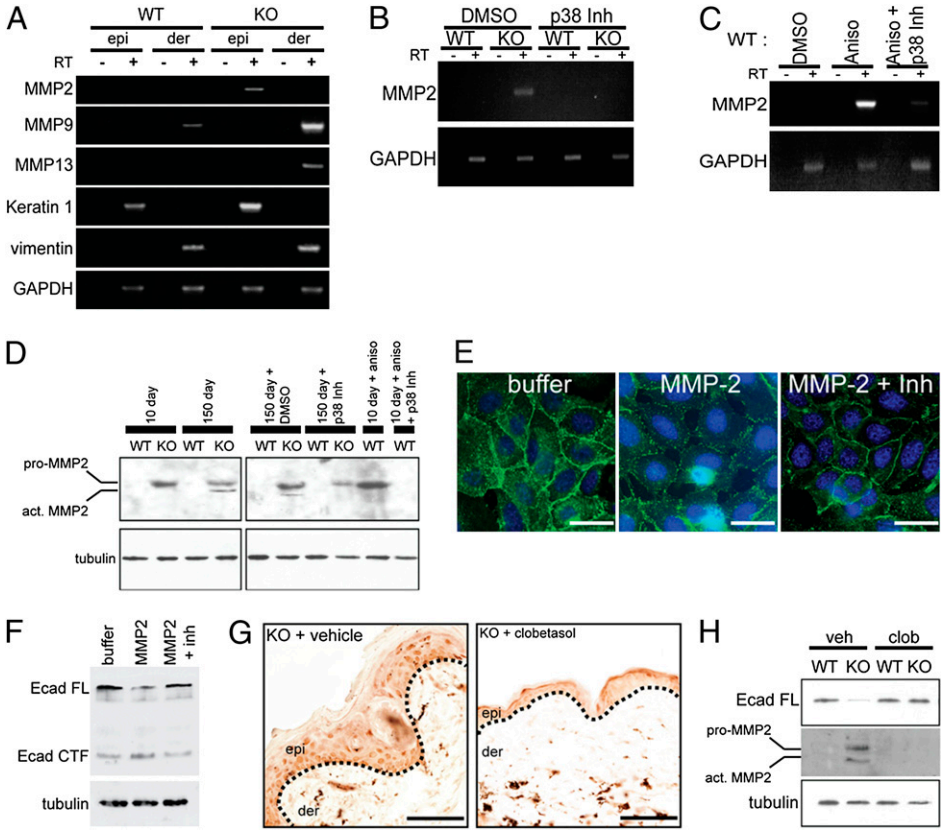

Fig. 5. MMP-2 expression and function. (*A*–*C*) RT-PCR using GAPDH as a loading control of five animals of each genotype performed in triplicate. (*A*) Expression of MMP-2, MMP-9, MMP-13, and keratin 1 and vimentin in postnatal day 10 WT versus KO skin. (*B*) Effect of p38 MAPK inhibitor on MMP-2 expression in postnatal day 10 skin. (*C*) Ability of the p38 MAPK chemical activator anisomycin to induce MMP-2 expression in WT epidermis. (*D*) Western blot of MMP-2 protein under conditions listed in *B* and *C* in young (10 d) and adult (150 d) mouse. (*E*) Effect of MMP-2 activity on adherens junctions in keratinocytes in vitro. E-cadherin is labeled in green and the nuclei labeled with DAPI is in blue. Keratinocytes were treated with buffer, recombinant MMP-2, or MMP-2 plus MMP-2 inhibitor (Inh). (Scale bars, 30 μm.) (*F*) Western blot of lysates made from cells treated with MMP-2 inhibitor using an antibody that recognizes Ecad FL and Ecad CTF following cleavage of the protein. Tubulin was used as a loading control. (*G*) Immunohistochemistry of phosphorylated p38 MAPK in KO skin from young mice treated with vehicle control or clobetasol. Dotted line denotes the basement membrane separating the epidermis (epi) from the dermis (der). (*H*) Western blot of Ecad FL, MMP-2, and tubulin of adult WT and KO skin treated with vehicle control of clobetasol.

mouse, whereas spongiosis is among the first histological signs in AD. We attribute this difference to the delay in the activation of MMP-2 zymogen even though the protein is present in young mice (Fig. 5).

The absence of caspase-8 appears to promote the pathogenesis of AD through the usurping of the inflammatory and proliferative phases of the wound healing response. Many diseases arise from the perturbation of a physiological process, and we postulate that the chronic repression of caspase-8 RNA in AD may result from a mutation in the transcriptional repressor of caspase-8, which renders it constitutively active. Alternatively, it is tempting to speculate that the factors that restore the homeostatic expression of epidermal caspase-8 following wound closure may be malfunctioning in AD skin. Whatever the rationale for repressing caspase-8 RNA in human AD skin may be, an important question is whether this down-regulation of caspase-8 is a cause or a consequence of the disease. Based on the fact that simply removing epidermal caspase-8 from the skin is able to recapitulate many of the cardinal features of AD led us to the conclusion that the loss of caspase-8 plays a causal role in this disease.

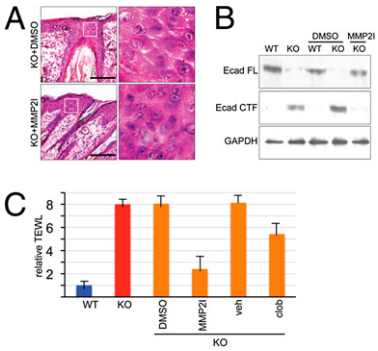

Fig. 6. Role of MMP-2 in the spongiotic phenotype (*A*) H&E staining of skin sections from adult KO mice injected with DMSO (KO + DMSO) vehicle control or MMP-2 inhibitor (KO + MMP2I). (*Right*) Magnified views of the boxed area (*Left*). (Scale bars, 30 μm.) (*B*) Western blot of proteins extracted from skin samples in *A*. Ecad FL and Ecad CTF were detected with an antibody recognizing both forms of the protein, and GAPDH was used as a loading control. (*C*) TEWL on adult WT and KO mice and KO mice treated with DMSO, MMP-2 inhibitor (MMP2I), vehicle control (veh), or clobetasol (clob). Results are representative of three independent experiments with three readings taken on the back skin per mouse. Error bars indicate SEM.

An interesting issue that arises from the parallels between AD and a chronic wound healing state is the participation of the inflammatory caspases, and in particular caspase-1. We previously demonstrated that caspase-1 is up-regulated in both wounds and the C8 cKO mouse, and this protein plays an important role in the maturation of inflammatory cytokines as a component of the inflammasome (3). Given its critical role in establishing the inflammatory microenvironment, which in turn stimulates epithelial stem cell proliferation, and tissue remodeling [partly through TSLP production (Fig. 4 *E* and *F*) and p38 MAPK activation (Fig. 5)], caspase-1 appears to be an attractive therapeutic target to combat the symptoms of AD. However, s.c. injection of a caspase-1 inhibitor into symptomatic C8 cKO skin does not diminish the acanthotic or spongiotic phenotypes (Fig. S7*A*), nor does it decrease the amount of TEWL (Fig. S7*B*). We conclude that caspase-1 may play a crucial role in the establishment of the inflammatory microenvironment but becomes dispensable in the chronic stages of AD.

Although the temporal appearance of spongiosis differs between the C8 cKO mouse model and human AD skin, the mechanisms involved in its manifestation are likely conserved. Spongiosis occurs in multiple human diseases and has long been assumed to be the result of excess fluid in the tissue (i.e., edema).

In fact, the disruption of adherens junctions has thought to be secondary to edema (26). However, there are skin diseases such as urticaria (i.e., hives), which have edema, but do not generally display a spongioform epidermis (27). This suggests that other factors are operating to shed E-cadherin, leading to intercellular gaps. In addition to edema, reports in the literature attribute E-cadherin shedding to apoptosis (28). However, the spongiotic epidermis of the C8 cKO mouse does not exhibit nuclear blebbing (Fig. 4*A*), a classic marker of apoptosis.

We found that E-cadherin shedding, and the spongiotic phenotype in the C8 cKO mouse, are significantly impacted by MMP-2 protease activity. Moreover, inhibition of MMP-2 activity in vivo is able to substantially reduce TEWL. The remaining water loss that occurred is likely caused by the reduction in the amount of filaggrin, which is required for proper barrier formation. When it has been activated, MMP-2 is sufficient to shed E-cadherin assembled in adherens junctions in cultured keratinocytes (Fig. 5*D*). Thus, it appears that spongiosis is an exaggeration of the remodeling phase of the wound, which likewise includes p38 MAPK activation (3, 29), MMP-2 expression (30), and remodeling of adherens junctions to facilitate reepithelialization. Overall, the use of the C8 cKO mouse to understand the molecular basis of AD has identified unappreciated mechanisms underlying this disease, which can be targeted for therapeutic intervention in patients.

Materials and Methods

Mice. The conditional deletion of epidermal caspase-8 was previously described (3). All animal work was carried out in accordance with the guidelines of University of California, San Diego, Institutional Animal Care and Use Committee. KO mice were injected s.c. with 200 μL of DMSO in PBS solution or 3 μM MMP2 inhibitor (EMD) daily for 4 d at phenotypic sites on the skin. Clobetasol propionate treatment was previously described (10).

Human Skin Samples. The protocol used to obtain human skin was approved by the Human Research Protection Program at University of California, San Diego. The atopic subjects had moderate to severe AD with an average Rajka–Langeland score of 6 (range, 4–9).

Tissue Analysis. Skin slices (10 μM) were sectioned from either optimal cutting temperature (OCT) compound (Tissue Tek) or paraffin (Richard Allan Scientific)–embedded samples and processed for staining. Antibodies and histological chemicals were previously reported (3).

Images were acquired on an Olympus Bx51 microscope with an Olympus DP70 camera. Acquisition were performed using a 40× 1.3 UPlan FL N objective (Olympus).

PCR. RNA was extracted from the skin of mice and cDNA synthesized as previously described (3). Primers sets were mined from the literature and are available upon request. Results are representative of at least three different experiments performed in triplicate.

Serum Ig Levels. The IgG1 and IgE ELISA kits were purchased from Southern Biotech and Biolegend, respectively, and used according to the manufacturers' protocols. IgG1 was measured in mg/mL and IgE in μg/mL.

TEWL. TEWL was measured on the dorsal skin of shaved mice by using s DPM 9003 device (Nova Technology). Measurements were performed at room temperature and results were recorded when TEWL regions stabilized. Three readings on the dorsal skin were taken on each mouse and averaged.

MMP-2 Activity. Recombinant human MMP-2 was purchased from R&D Systems and activated according to the manufacturer's instructions except that Brij-35 was deleted from the protocol. Activated MMP-2 (10 ng) in 50 μL of buffer was added to primary mouse keratinocytes grown on glass coverslips and incubated at 37 °C for 1 h. Keratinocytes were fixed for immunofluorescence or were lysed to perform a Western blot.

ACKNOWLEDGMENTS. We thank Edward Yang, Drs. Benjamin Yu, Yann Kerdiles, and David Stachura, and members of the C.J. laboratory for insightful discussions and technical assistance, and the laboratories of Drs. Richard Firtel, Stephen Hedrick, and Eduardo Macagno (all from the University of California at San Diego, La Jolla, CA) for reagents and use of equipment. S.L. is supported by a National Science Foundation predoctoral fellowship. P.L. is supported by a National Research Service Award [National Institute of Arthritis and Musculoskeletal and Skin Diseases (NIAMS) Grant 5F31AR056593-02]. C.J. is supported by a Hellman Faculty Fellowship. Work in the C.J. laboratory was funded by grants from the National Institutes of Health (NIAMS Grant 5R01AR053185-03) and by the American Cancer Society.

1. Mueller MM (2006) Inflammation in epithelial skin tumours: Old stories and new ideas. *Eur J Cancer* 42:735–744.
2. Schäfer M, Werner S (2008) Cancer as an overhealing wound: An old hypothesis revisited. *Nat Rev Mol Cell Biol* 9:628–638.
3. Lee P, et al. (2009) Dynamic expression of epidermal caspase 8 simulates a wound healing response. *Nature* 458:519–523.
4. Chun HJ, et al. (2002) Pleiotropic defects in lymphocyte activation caused by caspase-8 mutations lead to human immunodeficiency. *Nature* 419:395–399.
5. Bieber T (2008) Atopic dermatitis. *N Engl J Med* 358:1483–1494.
6. Williams H, Flohr C (2006) How epidemiology has challenged 3 prevailing concepts about atopic dermatitis. *J Allergy Clin Immunol* 118:209–213.
7. Grewe M, et al. (1998) A role for Th1 and Th2 cells in the immunopathogenesis of atopic dermatitis. *Immunol Today* 19:359–361.
8. Scharschmidt TC, Segre JA (2008) Modeling atopic dermatitis with increasingly complex mouse models. *J Invest Dermatol* 128:1061–1064.
9. Kovalenko A, et al. (2009) Caspase-8 deficiency in epidermal keratinocytes triggers an inflammatory skin disease. *J Exp Med* 206:2161–2177.
10. Aberg KM, et al. (2007) Psychological stress downregulates epidermal antimicrobial peptide expression and increases severity of cutaneous infections in mice. *J Clin Invest* 117:3339–3349.
11. Schmidt-Weber CB, Akdis M, Akdis CA (2007) TH17 cells in the big picture of immunology. *J Allergy Clin Immunol* 120:247–254.
12. Bonecchi R, et al. (1998) Differential expression of chemokine receptors and chemotactic responsiveness of type 1 T helper cells (Th1s) and Th2s. *J Exp Med* 187: 129–134.
13. Pivarcsi A, Homey B (2005) Chemokine networks in atopic dermatitis: traffic signals of disease. *Curr Allergy Asthma Rep* 5:284–290.
14. Tanaka T, et al. (2001) Interleukin-18 is elevated in the sera from patients with atopic dermatitis and from atopic dermatitis model mice, NC/Nga. *Int Arch Allergy Immunol* 125:236–240.
15. Konishi H, et al. (2002) IL-18 contributes to the spontaneous development of atopic dermatitis-like inflammatory skin lesion independently of IgE/stat6 under specific pathogen-free conditions. *Proc Natl Acad Sci USA* 99:11340–11345.
16. Hamid Q, et al. (1996) In vivo expression of IL-12 and IL-13 in atopic dermatitis. *J Allergy Clin Immunol* 98:225–231.
17. Damsgaard TE, Olesen AB, Sørensen FB, Thestrup-Pedersen K, Schiøtz PO (1997) Mast cells and atopic dermatitis. Stereological quantification of mast cells in atopic dermatitis and normal human skin. *Arch Dermatol Res* 289:256–260.
18. Werfel T, Kapp A (1998) Environmental and other major provocation factors in atopic dermatitis. *Allergy* 53:731–739.
19. Stenn KS, Balin AK, Higgins T, Stenn JO (1981) Spongiosis. *J Am Acad Dermatol* 5: 213–214.
20. Jamora C, Fuchs E (2002) Intercellular adhesion, signalling and the cytoskeleton. *Nat Cell Biol* 4:E101–E108.
21. Palmer CN, et al. (2006) Common loss-of-function variants of the epidermal barrier protein filaggrin are a major predisposing factor for atopic dermatitis. *Nat Genet* 38: 441–446.
22. Demehri S, et al. (2008) Notch-deficient skin induces a lethal systemic B-lymphoproliferative disorder by secreting TSLP, a sentinel for epidermal integrity. *PLoS Biol* 6:e123.
23. Bogiatzi SI, et al. (2007) Cutting edge: Proinflammatory and Th2 cytokines synergize to induce thymic stromal lymphopoietin production by human skin keratinocytes. *J Immunol* 178:3373–3377.
24. Giannelli G, et al. (2002) Gelatinase expression at positive patch test reactions. *Contact Dermat* 46:280–285.
25. Han J, Lee JD, Bibbs L, Ulevitch RJ (1994) A MAP kinase targeted by endotoxin and hyperosmolarity in mammalian cells. *Science* 265:808–811.
26. Trautmann A, et al. (2001) The differential fate of cadherins during T-cell-induced keratinocyte apoptosis leads to spongiosis in eczematous dermatitis. *J Invest Dermatol* 117:927–934.
27. Nichols KM, Cook-Bolden FE (2009) Allergic skin disease: Major highlights and recent advances. *Med Clin North Am* 93:1211–1224.
28. Akdis CA, et al.; European Academy of Allergology; Clinical Immunology/American Academy of Allergy, Asthma and Immunology/PRACTALL Consensus Group (2006) Diagnosis and treatment of atopic dermatitis in children and adults: European Academy of Allergology and Clinical Immunology/American Academy of Allergy, Asthma and Immunology/PRACTALL Consensus Report. *Allergy* 61:969–987.
29. Kobayashi H, Aiba S, Yoshino Y, Tagami H (2003) Acute cutaneous barrier disruption activates epidermal p44/42 and p38 mitogen-activated protein kinases in human and hairless guinea pig skin. *Exp Dermatol* 12:734–746.
30. Kähäri VM, Saarialho-Kere U (1997) Matrix metalloproteinases in skin. *Exp Dermatol* 6:199–213.

Supporting Information

Li et al. 10.1073/pnas.1009751108

SI Materials and Methods

Mice. The conditional deletion of epidermal caspase-8 was engineered by mating mice with floxed alleles of exon 3 of caspase-8 (1) with transgenic mice harboring Cre recombinase under the control of the keratin 14 promoter (2). Mice were analyzed at postnatal day 10, 15, or 150. Clobetasol propionate (0.05%) or propylene glycol/ethanol (7:3 vol/vol) vehicle was topically applied to the phenotypic skin twice daily for 10 d.

For tissue analysis, mouse skins were frozen in OCT compound (Tissue-Tek) or fixed overnight in Bouin fixative and embedded in paraffin, depending on the application. Skin sections were cut on a cryostat (HM 525; Microm) or microtome (RM2165; Leica). For immunohistochemistry, secondary antibodies conjugated to rhodamine-X, FITC, or HRP (Jackson Immunoresearch) were used. HRP signals were developed using Vectastain ABC skit (Vector Labs) according to the manufacturer's protocol. H&E (Richard Allan Scientific) staining and Toluidine blue (Sigma) staining were carried out on paraffin-embedded sections.

Human Skin Samples. Skin biopsy samples (2 mm) were collected from patients with AD at University of California, San Diego. The atopic subjects had moderate to severe AD with an average Rajka–Langeland score of 6 (range, 4–9). For all procedures, informed consent was obtained. After the injection of local anesthesia, 2-mm punch biopsy specimens were taken from the untreated skin of individuals with AD and from normal volunteers as a control. Samples were embedded in OCT compound and stored at −20 °C until use or incubated in TRIzol (Invitrogen) for RNA extraction. Quantitative PCR of these samples was performed and transcript values were normalized according to the expression of the housekeeping gene GAPDH. Caspase-8 levels in normal skin were normalized to 1. Caspase-8 expression in AD samples are expressed relative to this value.

PCR. Total RNA was extracted from whole skin of WT and KO mice using TRIzol reagent (Invitrogen) according to manufacturer instructions. Similarly, epidermis from WT and KO mice was separated with dispase treatment for 1 h at 37 °C and total RNA was isolated using the TRIzol protocol. cDNA was synthesized by reverse transcription using oligo-dT as primers (Superscript III kit; Invitrogen). Real-time PCR analysis was performed with previously described primers using the BioRad CFX96 quantitative PCR machine. Reactions were performed using the SSOFast EvaGreen Master mix (BioRad) and experiments were carried out in triplicate from cDNA isolated from at least three different animals. Data shown are a representative example. The specificity of reactions was determined by dissociation curve analysis and quantification analysis was performed using the Mx-3000 software. For RT-PCR reactions, cDNA was amplified in a BioRad iCycler using 30 to 35 cycles and visualized on an ethidium bromide containing agarose gel.

Measurement of Cytokine Levels. The amount of various cytokines secreted from the epidermis or found in the serum was determined by ELISA using kits from R&D Systems. Epidermal explants were extracted with dispase as described earlier and incubated with keratinocyte media overnight. This conditioned media was then used in the ELISA protocols. Equalization of starting material was carried out by quantifying the amount of actin from each explant and results of the ELISA were divided by this value. To measure cytokine amounts in the serum, blood was extracted from the cheek of the mice and allowed to coagulate for 1 h. The sample was gently centrifuged to separate the cells from the serum and the latter was used in the ELISA kit immediately upon separation from the blood cells.

1. Beisner DR, Ch'en IL, Kolla RV, Hoffmann A, Hedrick SM (2005) Cutting edge: Innate immunity conferred by B cells is regulated by caspase-8. *J Immunol* 175: 3469–3473.

2. Vasioukhin V, Degenstein L, Wise B, Fuchs E (1999) The magical touch: Genome targeting in epidermal stem cells induced by tamoxifen application to mouse skin. *Proc Natl Acad Sci USA* 96:8551–8556.

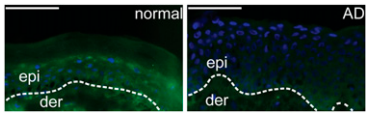

Fig. S1. Immunofluorescence of caspase-8 (green) in normal and AD human skin. Nuclei are stained with DAPI. The white dotted line denotes the basement membrane separating the epidermis (epi) from the dermis (der). (Scale bar, 30 μm.)

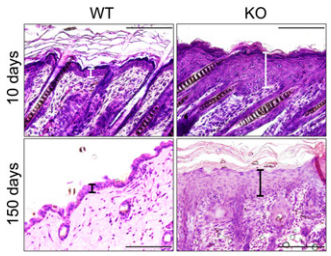

Fig. S2. H&E staining of WT and epidermal caspase-8 KO skin from 10-d- and 150-d-old mice. epi, epidermis; der, dermis; hf, hair follicle. Vertical bars denote thickness of epidermis from the basement membrane through the granular layer. (Scale bar, 30 μm.)

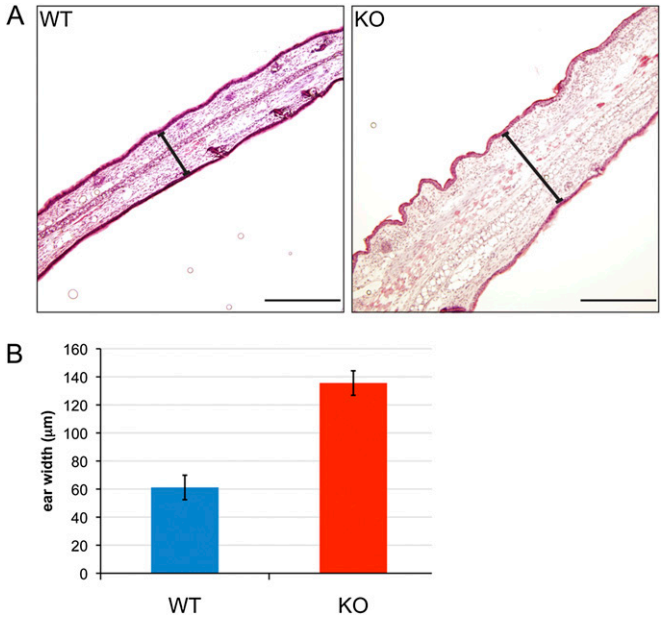

Fig. S3. Evidence for cutaneous edema. (*A*) Sections of the ears from 10-d-old WT and caspase-8 KO mice were stained with H&E. Dermal thickness is denoted by the bar. (*B*) Quantitation of average ear thickness. Data are the aggregate of 10 random measurements on six different ears.

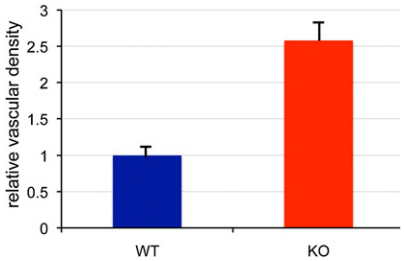

Fig. S4. Quantitation of vascular density in the skin. Amount of CD31 staining was quantified as a percentage of dermal area. Results are from five random fields with a 10× objective and WT was normalized as 1. At least three different mice were used to quantify vascular density.

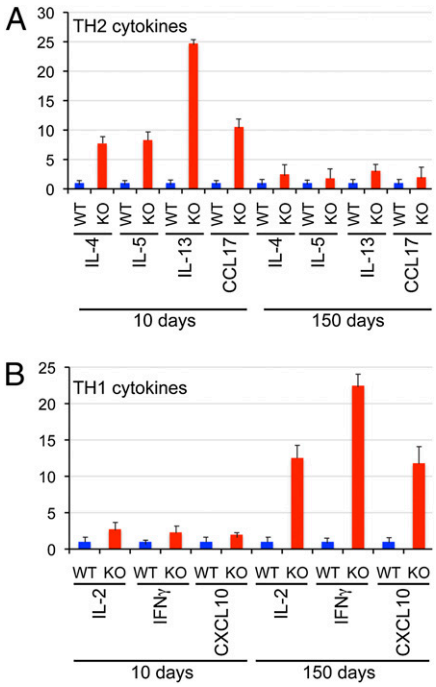

Fig. S5. Quantitation of secreted cytokines. Skin from 10-d- or 150-d-old WT or KO mice were used to condition media overnight. The media was then used to measure the amount of secreted TH2 signature cytokines (*A*) and TH1 signature cytokines (*B*). Results are the average of at least three different samples for each age and genotype repeated in triplicate. WT levels were normalized to 1.

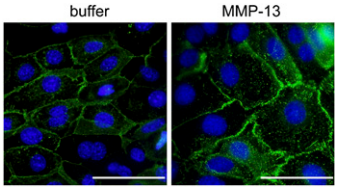

Fig. S6. Effect of MMP-13 on adherens junctions. Primary mouse keratinocytes were treated with buffer or MMP-13 for 2 h at 37 °C. Cells were fixed and stained with E-cadherin (green) or DAPI (blue).

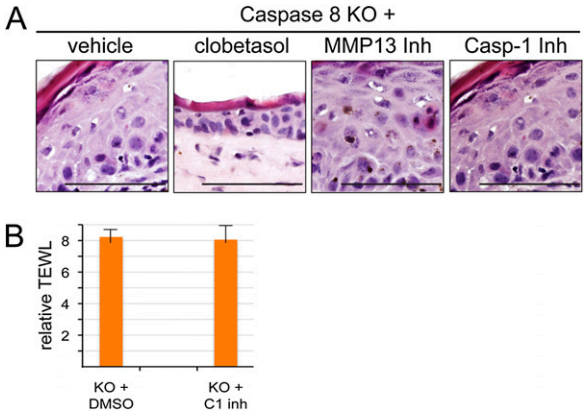

Fig. S7. Effect of inhibitors on spongiosis. (*A*) Adult caspase-8 KO mice were treated with vehicle, clobetasol, MMP-13 inhibitor (MMP13 Inh), or caspase-1 inhibitor (Casp-1 Inh) and stained with H&E. (*B*) TEWL was measured in adult KO mice treated with DMSO or caspase-1 inhibitor. Results are the average of three different readings on the same mouse, with three mice for each treatment.

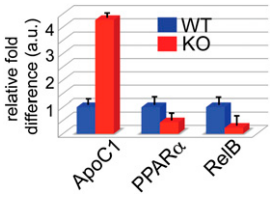

Fig. S8. C8 cKO skin recapitulates genetic changes found in other mouse models of AD. Several mouse models have been engineered that exhibit certain features of AD. For instance, transgenic overexpression of caspase-1, which proteolytically activates IL-1β (1), and ApoC1, an apolipoprotein involved in lipoprotein metabolism (2), are reported models for AD. We previously found that caspase-1 is up-regulated in the caspase-8–null mouse (3) and also observe an elevated level of ApoC1. Furthermore, genetic ablation of the transcription factors RelB (4), a member of the NF-κB/Rel family, and PPAR-α (5), which belongs to the nuclear receptor superfamily, likewise produce defects consonant with AD and both are significantly reduced in the mouse lacking epidermal caspase-8.

1. Yamanaka K, et al. (2000) Skin-specific caspase-1-transgenic mice show cutaneous apoptosis and pre-endotoxin shock condition with a high serum level of IL-18. *J Immunol* 165: 997–1003.
2. Nagelkerken L, et al. (2008) Development of atopic dermatitis in mice transgenic for human apolipoprotein C1. *J Invest Dermatol* 128:1165–1172.
3. Lee P, et al. (2009) Dynamic expression of epidermal caspase 8 simulates a wound healing response. *Nature* 458:519–523.
4. Freyschmidt EJ, et al. (2007) Skin inflammation in RelB(-/-) mice leads to defective immunity and impaired clearance of vaccinia virus. *J Allergy Clin Immunol* 119:671–679.
5. Staumont-Salle D, et al. (2008) Peroxisome proliferator-activated receptor alpha regulates skin inflammation and humoral response in atopic dermatitis. *J Allergy Clin Immunol* 121: 962–968.

Table S1. Summary of caspase-8 KO phenotype

	Age 5 d		Age 10 d		Age 90 d		Age 150 d	
Characteristic	WT	KO	WT	KO	WT	KO*	WT	KO*
Epidermal thickness, μm	41 ± 7.8	67.4 ± 10.2	33 ± 4.7	86 ± 15.3	22 ± 5.8	55 ± 11.29	20 ± 4.6	59.6 ± 22.1
T_H2 (normalized)								
IL-4	1.0 ± 0.05	4.7 ± 0.4	1.0 ± 0.04	5.1 ± 0.3	1.0 ± 0.06	2.7 ± 0.1	1.0 ± 0.08	3.2 ± 0.2
IL-5	1.0 ± 0.03	3.5 ± 0.2	1.0 ± 0.05	5.7 ± 0.2	1.0 ± 0.05	2.1 ± 0.2	1.0 ± 0.06	1.3 ± 0.1
IL-13	1.0 ± 0.03	10 ± 1.1	1.0 ± 0.04	32 ± 2.1	1.0 ± 0.07	3.5 ± 0.4	1.0 ± 0.09	4.7 ± 0.4
T_H1 (normalized)								
IFNγ	1.0 ± 0.02	1.1 ± 0.2	1.0 ± 0.03	1.8 ± 0.5	1.0 ± 0.01	4.1 ± 0.5	1.0 ± 0.05	3.8 ± 0.2
IL-18	1.0 ± 0.03	0.9 ± 0.3	1.0 ± 0.02	1.9 ± 3	1.0 ± 0.05	10 ± 2.7	1.0 ± 0.04	12 ± 1.1
Mast cells/10 mm^2	49.5 ± 12	51 ± 8.4	43 ± 6.89	81.5 ± 10.4	40.7 ± 6.89	215 ± 10.1	53.8 ± 7.9	256 ± 13.8
Serum IgG1, mg/mL	0.25 ± 0.03	0.49 ± 0.09	0.3 ± 0.02	0.86 ± 0.16	0.29 ± 0.05	1.38 ± 0.32	0.36 ± 0.06	1.84 ± 0.32
Serum IgE, μg/mL	0.1 ± 0.03	0.05 ± 0.01	0.07 ± 0.02	0.1 ± 0.05	0.05 ± 0.01	0.96 ± 0.06	0.08 ± 0.03	2.39 ± 0.19
Spongiosis	None	None	None	None	None	Present	None	Present
E-cad FL (normalized)	1	0.95 ± 0.08	1	0.92 ± 0.07	1	0.75 ± 0.08	1	0.47 ± 0.04
E-cad CTF (normalized)	1	0.9 ± 0.13	1	1.2 ± 0.15	1	1.5 ± 0.22	1	2.3 ± 0.46
Filaggrin (normalized)	1	1.1 ± 0.06	1	1.1 ± 0.03	1	0.8 ± 0.18	1	0.5 ± 0.15
TEWL, g/h^2	87 ± 5	92 ± 9	89 ± 5	88 ± 7	95 ± 8	832 ± 23	88 ± 10	986 ± 13
MMP2 RNA	ND	Present	ND	Present	ND	Present	ND	Present

ND, not detected. Data presented are from ≥ 5 mice. The 90-d- and 150-d-old mice were mosaic and the analysis of the skin was done on phenotypic regions. The visible phenotypes in these adult mice developed along the same timeframe as the young mice.
*Phenotypic region.